Lab on a Chip

PAPER

View Article Online
View Journal



Cite this: DOI: 10.1039/c5lc00547g

# Asphaltenes yield curve measurements on a microfluidic platform

Vincent J. Sieben, Asok Kumar Tharanivasan, John Ratulowski and Farshid Mostowfi*

We describe a microfluidic apparatus and method for performing asphaltene yield measurements on crude oil samples. Optical spectroscopy measurements are combined with a microfluidic fluid handling platform to create an automated microfluidic apparatus to measure the asphaltene yield. The microfluidic measurements show good agreement with conventional wet chemistry measurements as well as available models. The initial absorbance of the oil is measured, and asphaltenes are removed from the oil by the gradual addition of *n*-alkane, which leads to flocculation and subsequent filtration. The absorbance of the de-asphalted oil (maltenes) is then measured and the initial asphaltene content is determined by the change in absorbance. The solubility of asphaltene is evaluated by varying the titrant-to-oil ratio (*e.g.*, *n*-heptane–oil), which induces no, partial, or full precipitation of asphaltenes depending on the chosen ratio. The absorbance of the filtrate is measured and normalized to the maximum content to determine the fractional precipitation at each ratio. Traditionally, a yield curve comprised of 20 such ratios would require weeks to months to generate, while consuming over 6 L of solvent and more than 100 g of crude oil sample. Using the microfluidic approach described here, the same measurement can be performed in 1 day, with 0.5 L of solvent and 10 g of crude oil sample. The substantial reduction in time and consumables will enable more frequent asphaltene yield measurements and reduce its environmental impact significantly.

Received 14th May 2015,
Accepted 19th August 2015

DOI: 10.1039/c5lc00547g

www.rsc.org/loc

## Introduction

Asphaltene precipitation and deposition is a major impediment in production, transportation and processing of reservoir fluids. Unexpected precipitation and the subsequent potential for deposition of asphaltenes can cause reservoir impairment, plugging of wells and flowlines, as well as fouling issues and processing challenges for surface facilities.[1] However, the mechanisms of agglomeration and deposition are not fully proven,[1,2] with only a few available predictive models.[3] Asphaltenes are a sub-component of crude oil that are conventionally defined as being poorly soluble in *n*-alkanes (*e.g. n*-heptane), and highly soluble in aromatic solvents (*e.g.* toluene).[4] Asphaltenes precipitate due to a shift in solubility matrix caused by a change in pressure, temperature, or composition of the oil.[5–8] For example, simply combining two incompatible oils may initiate precipitation through a change in composition; even though, both stand-alone samples have asphaltene fractions that otherwise remain stable in solution.[9,10] Optimal flow assurance requires frequent and accurate fluid characterization and asphaltene phase behavior studies for each crude sample. Quantitative measurements that describe the degree of asphaltene precipitation in response to varying perturbations aid in understanding the general behavior of these diverse aggregates and help mitigate or prevent costly remedial techniques to remove the problematic material.

Asphaltenes are a complex mixture of different molecules with varying solubility parameters, ranging from least soluble or most unstable and first to precipitate, to most soluble or most stable and last to precipitate sub-fractions. The solubility profile of the asphaltene fraction is represented by a yield curve. A yield curve shows the amount of asphaltenes precipitated as the ratio of the solvent/precipitant mixture is changed. A number of techniques may be used to detect and measure the extent of asphaltene precipitation, including visual observation,[11] absorption and fluorescence spectroscopy,[12] light scattering,[6] conductivity,[13] filtration,[14] viscosity[15] and the conventional gravimetric approach.[16] Typically, the maximum asphaltene content of a crude oil is measured at a heptane–crude oil volume ratio of 40. As the amount of *n*-alkane (or titrant) is reduced, a fraction of the total amount of asphaltene precipitates while the remainder stays in solution due to partial solubility. An asphaltene yield curve is a graph that shows the amount of precipitated asphaltenes as a function of titrant concentration.[2] A yield curve contains

*Schlumberger Canada Limited, DBR Technology Center, 9450 17th Avenue, Edmonton, Alberta, T6N 1M9, Canada. E-mail: fmostowfi@slb.com; Tel: +1 780 577 8341*

valuable information about the solubility or phase separation of asphaltenes; notably the precipitation onset point, or the alkane-to-oil ratio at which asphaltene precipitation begins. Although the yield curve provides meaningful data for modelling asphaltene behavior,[4,5,17–19] the cost and time required to complete the analysis are generally prohibitive to be performed routinely using existing methods.

The applications of microfluidics in the oil and gas industry have grown substantially in recent years. Various methods for measuring asphaltene content/properties,[20–25] phase behavior,[26–28] gas–oil ratio,[29] solvent diffusion[30,31] and micromodels[32,33] have been published, uncovering a completely new field of relevance for microfluidic research. Bowden *et al.* demonstrated one of the first separations of asphaltenes on a microfluidic chip.[22,23] In their early work, they fractionated hydrocarbons using an H-cell microfluidic platform so they could rapidly and continuously mix the oil with hexane. The device allowed the removal of the high molecular weight species from the apolar components that could then be directly used on a GC.[22] Although Bowden *et al.* was initially interested in the lighter fractions of the oil (free of asphaltenes), they remarked on the potential utility of microfluidics to evaluate the solubility of asphaltenes analogous to precipitation onset titration. The later work by Bowden *et al.* coupled UV-vis spectroscopy with the H-cell microfluidic device to determine the asphaltene content and carboxylic acid content, demonstrating the potential utility of microfluidics for characterization of oil composition.[23] At nearly the same time, Mostowfi *et al.* were also investigating an approach to determine asphaltene content using UV-vis absorbance, and comparing the optical data to the traditional ASTM D6560 (IP 143) method for 26 crude oil samples.[34] The data showed a strong linear correlation between optical absorbance and asphaltene content for a large sample set that covered a wide range of geographic locations. Schneider *et al.* combined the optical technique with a microfluidic platform for rapid asphaltene content measurement on 38 crude oil samples, and demonstrated that a single asphaltene content measurement could be made in less than 30 minutes as opposed to days.[20] Sieben *et al.* continued the work, expanding to 52 crude oil samples with a larger operating range capable of measuring asphaltene contents up to 15 wt%.[24] Recent work by Hu and Hartman utilize microfluidics to investigate deposition of asphaltenes in porous media or packed bed reactors (PBR).[21,25] By coupling optical analysis (UV-vis) to a micro-PBR, they were able to study the influence of Reynolds number on asphaltene deposition in a rapid manner. Microfluidics has been successfully applied for the separation of asphaltenes, the measurement of asphaltene content and recently the study of asphaltene aggregation and deposition behavior.

In this work, an optical microfluidic apparatus and method for asphaltene content measurement described earlier,[20,24,34] is augmented to perform solubility measurements (yield curve). The underlying principles of the optical detection have been addressed in previous work,[34] where it was established that asphaltene optical absorbance in the visible range correlated linearly with conventional asphaltene weight measurements based on ASTM D-6560.[35] Briefly, the initial absorbance of the oil is measured before asphaltenes are precipitated. Next, the addition of excess *n*-alkane (*e.g.* *n*-heptane) induces asphaltene precipitation and the aggregates are filtered out of solution. Subsequently, the absorbance of the de-asphalted oil (*i.e.*, maltenes) is measured and the maximum asphaltene content is determined by the change in absorbance through the established correlation.[20,34] The ability to rapidly measure asphaltene content using the microfluidic approach may remove the throughput bottlenecks associated with conventional yield curve measurements.

Here, we extend the functionality of the microfluidic asphaltene measurement by varying the titrant–oil ratio to evaluate the solubility of asphaltenes. When *n*-heptane is mixed with an oil sample at various ratios, it will induce a partial or fractional precipitation of asphaltene, depending on the chosen ratio. Mixing of oil with *n*-heptane is achieved using a microfluidic mixer which employs a static mixing principle based on fluid lamination and diffusion. After mixing, the fluid is passed through a long microfluidic channel referred to as "reactor". This channel allows sufficient time for the potential precipitation of adequately sized asphaltene particles before the fluid stream reaches the filtration unit. While the microfluidic chip contains the core functionality of mixing the fluids, precipitating asphaltenes and filtering the precipitate, peripheral equipment are required in order to drive and condition the fluids, and perform the optical analysis. As shown in Fig. 1, the oil sample is loaded manually in the sample loop from where it can be automatically pushed into the microfluidic chip by a toluene-filled syringe. A second syringe dispenses *n*-heptane into the core microfluidic chip at a particular flow rate matched to the sample-pushing flow rate so that the desired mixing ratio is achieved. Heptane and the oil sample are combined on the microfluidic chip in the mixer section, which might cause some or all asphaltenes to precipitate, depending on the mixing ratio. Asphaltene aggregates are held back in the subsequent filtration section while the permeate is guided towards a second mixing chip, based on the same mixing principles as described above. Fig. 1B is a photograph of the designed core microfluidic chip used in this study. Fig. 1C shows a photograph of the chip while asphaltene particles are precipitating in the channel.

The second mixer unit is an important addition to the previous work described in ref. 20, which was originally designed for high dilutions (*i.e.* addition of excess *n*-heptane to oil provides sufficient dilution for optical measurement). However, in this work, measurements are made at low dilution ratios to establish the complete yield curve. At a low heptane dilution, the permeate is predominantly a dark fluid which produces exceedingly high optical absorbance values for the fixed pathlength of the flow cell. Hence, the dark permeate is diluted with an adequate amount of toluene so that the absorbance of the deasphalted oil at low dilution ratios is within the spectrometer's detectable range. The output from

 

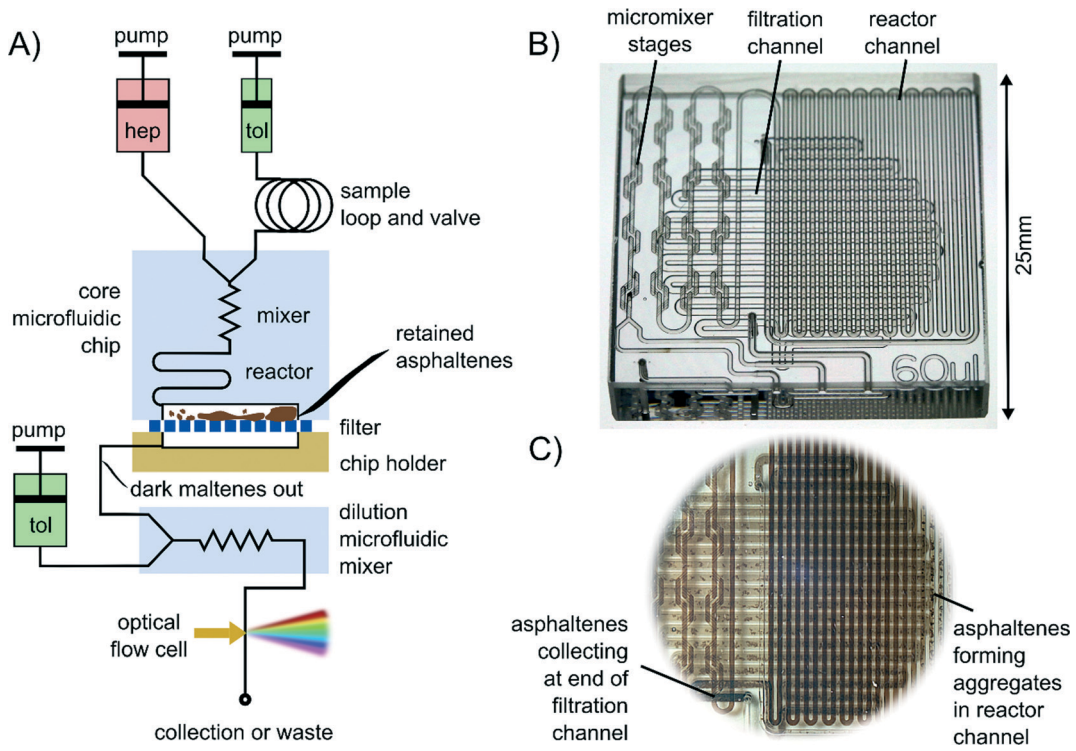


**Fig. 1** A) Simplified flow diagram to obtain an asphaltene precipitation yield curve using a microfluidic system; the filtration aspects of the chip are shown in a cross-sectional view. Crude oil and heptane are mixed at a user-selected volumetric ratio and asphaltenes precipitate in the reaction unit. Asphaltene aggregates are screened by the filter membrane on the lower level of the chip. Permeate is then diluted with toluene if required and the optical absorption is measured. B) Core microfluidic chip: photograph of an empty glass chip containing the mixer, reactor and filter channels. C) Photograph of the core chip embedded in the chip holder during operation; top view that shows that the asphaltenes are retained by the filter membrane (in the paper plane), and usually collected at the end of the filtration channel filling gradually to the inlet.

the second mixer stage (*i.e.* the diluted permeate) is then passed through the optical flow cell, where the absorbance spectrum of the fluid is measured. Based on the absorbance and the correlation relating absorbance and asphaltene content, the asphaltene yields for various heptane–oil ratios can be determined. The use of such microfluidic systems to perform resource intensive studies on asphaltene solubility will greatly improve data quality through automation and reduce the labor and time associated with conventional approaches.

## Methods and materials

### Sample set

Six stock tank oil samples were evaluated in this study, spanning a range of asphaltene contents as listed in table 1. Saturates, aromatics, resins and asphaltenes (SARA) contents for crude oils A, B and C were obtained from ref. 36. The SARA fractions for crude oils D, E and F were measured using a modified ASTM D6560 (IP 143) method and a modified ASTM D4124 method described elsewhere.[19,34] The solvents for the microfluidic asphaltene apparatus were HPLC-grade toluene (CAS # 108-88-3) and *n*-heptane (CAS # 142-82-5) purchased from Fisher Scientific (NJ, USA).

### Microfluidic chips

Two glass microfluidic chips were used in this study, both manufactured by Dolomite (Royston, UK). The first chip included a y-junction for introducing the oil sample and *n*-heptane (titrant), several micro-mixer stages to reduce cross-stream diffusion lengths, a serpentine reactor to induce a time delay for reaction kinetics, and an open-face filtration

**Table 1** Composition and densities of crude oils used in this study (1 atm and 20 °C)

| | | Composition (wt%) | | | | |
|---|---|---|---|---|---|---|
| Sample | °API | Saturates | Aromatics | Resins | *n*-C7 asphaltenes | Recovery |
| Crude oil A | 29.5 | 61.6 | 18.4 | 13.5 | 6.1 | 99.6 |
| Crude oil B | 16.5 | 38.4 | 29.8 | 25.8 | 6.8 | 100.8 |
| Crude oil C | 31.2 | 63.1 | 20.2 | 13.3 | 3.7 | 100.3 |
| Crude oil D | 29.4 | 50.3 | 24.8 | 22.6 | 1.1 | 98.8 |
| Crude oil E | 21.1 | 40.2 | 27.1 | 23.9 | 8.5 | 99.7 |
| Crude oil F | 28.5 | 54.4 | 21.9 | 18.8 | 4.3 | 99.4 |

channel that interfaced with porous membrane for filtration and removal of asphaltene aggregates. The filtered mixture was then fed into the second microfluidic chip, which incorporated a 3-way y-junction to further dilute the sample with toluene. The second chip also incorporated several micro-mixer stages for creating a homogeneous deasphalted oil–toluene mixture for downstream optical analysis. Conventional photolithography techniques were used to fabricate the microfluidic chips; *i.e.* lithography, isotropic etching and temperature annealing. Nominal cross-sectional dimensions of microchannels were (depth by width): 125 μm x 350 μm (large channels) and 50 μm x 125 μm (small channels) for the mixer stages; 250 μm x 370 μm for the reactor channel; 175 μm x 350 μm for interconnecting channels; and 200 μm x 600 μm for the open-faced (*i.e.* not capped) filtration channel. The first core chip had an internal volume of 51 μL plus a reactor section that could be 10, 20 or 60 μL depending on the design. The second dilution chip had an internal volume of 8 μL.

To ensure that oil and heptane are well mixed, the chip incorporates 16 micro-mixers that operate similarly to split and recombine mixers described by Nguyen and Wu.[37] These mixers cut down the inter-stream diffusion distances substantially and mixing occurs much more rapidly. In this particular mixer, the diffusion length is reduced 8 times after each mixer stage. For a typical flow rate of 80 μL $min^{-1}$, the manufacturer recommends 6 micro-mixer stages, which are much less than the number of stages incorporated in our device, thereby ensuring a well-mixed stream entering the reactor. We have confirmed a homogenous mixture with microscopy at a ratio of 40 : 1 (*n*-heptane–oil) after 4–8 mixer stages, far before entering the reactor.

The reactor length or volume is an important parameter to be considered as together with the flow rate it determines the residence time, *i.e.* the time the asphaltenes are allowed to precipitate after mixing with heptane and before the separation by filtration. In our previous work,[20] we showed that Taylor–Aris dispersion of oil sample plugs is a valid description of broadening as the plug traverses our microfluidic channels – indicating that the oil constituents are crossing the axial flow lines enough times to make the model valid. In other words, the cross-sectional diffusion time is sufficiently small compared to the axial transit time as the sample flows through the chip. Schneider *et al.* determined that asphaltenes diluted in excess toluene have a diffusion coefficient of around 5 x $10^{-6}$ $cm^2$ $s^{-1}$.[12] The calculated characteristic diffusion time across the reactor channel is approximately 0.8 seconds. Therefore, there is sufficient time for the diffusion of asphaltenes to form aggregates as the axial transit time is usually greater than 5 seconds.

### Complete system

A custom-made aluminum and polyether ether ketone (PEEK) block or chip holder was used to house the core microfluidic chip. The PEEK section of the chip holder had a micro-machined serpentine channel that was open-faced for permeate collection; it was a mirror image of the core chip filtration channel. The porous filter membrane was compressed between the core microfluidic chip and the PEEK portion of the chip holder as shown in Fig. 1A. The filter used in this work was a hydrophobic polytetrafluoroethene (PTFE) membrane with an average pore size of 0.2 μm for separating the precipitated asphaltenes from maltenes. ASTM standard D6560 recommends the use of WhatmanTM grade 42 filters, which would retain particles larger than 2.5 μm.[35] If microscopy methods are used, the precipitation onset is detected when the particle size is about 1 μm.[9] Hence, the nominal pore size of the filter (0.2 μm) used in this work is more stringent than traditional methods for detecting precipitation. The chip holder also created fluidic connections to external tubing for reagent delivery and collection. The total volume of the assembly was approximately 152 μL. For temperature control, the entire setup was placed inside a customized block heating system (QBD4, Grant, UK).

The output from the core chip holder assembly was routed to the second microfluidic chip for post-dilution with toluene. The toluene post-dilution provided a detectable absorbance on the fluids with no or low *n*-heptane dilution for spectrometric measurements, ensuring that the measured deasphalted oil absorbance was in the linear range with a value less than two.[38] The optical absorbance of the toluene-diluted permeate was measured with a 2.5 mm path length flow cell (SMA-Z-2.5-uvol, 2 μL internal volume, FIALABs, USA), using a tungsten halogen white-light source (LS-1, Ocean Optics, usable range 360–2500 nm) and a UV-VIS spectrometer (HR2000 + CG-UV-NIR, Ocean Optics, usable range 200–1100 nm).

Three stepper-motor syringe pumps (Mitos Duo XS, part #3200057, Dolomite, UK) were used to pump the toluene, *n*-heptane and the oil sample plug. Glass syringe sizes were selected based on the desired mixing ratios to maintain a smooth flow and minimize the number of syringe refills. Pressure sensors (40PC150G2A, Honeywell, USA) were used to ensure safe operation and also to verify that the automated protocol performed as anticipated. Sample plug loading and injection was accomplished with a rotary valve (Cheminert C22-3186EH, VICI-Valco, USA). Additional valves were used for fluid routing. The maximum operating pressure of the system was theoretically 10 bar, limited by the glass syringe, the valves and the filter membrane holder. The system was operated within 6 bar for reliability and safety reasons. The sample and the solvents were filtered using 10 μm and 2 μm in-line frit cartridges, respectively. When required, samples were pre-filtered with a 0.2 μm PTFE syringe filter to remove excess fines and particles. All fluidic components were connected using fluorinated ethylene propylene (FEP) tubing which had an inner diameter of 250 μm. The whole system operation was controlled and automated with custom electronics and a personal computer running the LabVIEW 8.6 (National Instruments, USA) software. The program also captured and analyzed the absorbance spectrum over time for data processing and presentation.

 

### Procedure

For each chosen *n*-heptane to oil volume ratio, a "run" is performed where *n*-heptane and oil are mixed, insoluble asphaltenes are precipitated and filtered, and the permeate is optionally diluted with toluene and passed through the spectroscopy flow cell, see Fig. 1 and 2. The post-dilution amount is determined by targeting for a final solvent dilution of about 40 : 1 (solvent : oil) based on the three pump flow rates. Flow conditions are maintained until a stable absorbance spectrum is acquired. Each run produces data corresponding to a single point on the asphaltene solubility curve (yield curve) and the entire curve is mapped out by multiple runs with various heptane to oil volume ratios. Hereafter, we define the heptane to oil volume ratio as the heptane–oil ratio (R).

Each yield curve contains an experimental run with a heptane–oil ratio near zero (neat oil, where most asphaltenes are soluble) and a run with maximum precipitation, often at a heptane–oil ratio of approximately 40. Based on these two key runs (no precipitation and maximum precipitation), the other data points are scaled and plotted as fractional asphaltene precipitation *versus* heptane–oil ratio, as in eqn (1):

$$x(R) = \frac{A_{\mathrm{asph}@R}}{A_{\mathrm{asph}@R_{\max}}} = \frac{A_{\mathrm{malt}@R=0} - A_{\mathrm{malt}@R}}{A_{\mathrm{malt}@R=0} - A_{\mathrm{malt}@R_{\max}}} \quad (1)$$

where $x(R)$ is the fractional asphaltene precipitation at the heptane–oil ratio $R$, $A_{\mathrm{asph}@R}$ is the asphaltene absorbance at $R$, $A_{\mathrm{asph}@R_{\max}}$ is the maximum asphaltene absorbance (usually around $R = 40$), $A_{\mathrm{malt}@R=0}$ is the absorbance of the filtrate when diluted in toluene (*i.e.* neat oil absorbance), $A_{\mathrm{malt}@R_{\max}}$ is the minimum filtrate absorbance at $R_{\max}$ (*i.e.* maximum asphaltene precipitation) and $A_{\mathrm{malt}@R}$ is the filtrate absorbance at the heptane–oil ratio $R$. Each absorbance value in eqn (1) is the difference between the absorbance value at wavelengths of 600 nm and 800 nm, as established in previous work.[34]

The characteristic absorbance for each heptane–oil ratio is adjusted to an equivalent solvent dilution of 40 : 1, based on the volumetric flow rates of the three syringes during a particular run. For example, at $R = 5$, the pump flow rates may be 75 μL min$^{-1}$ *n*-heptane, 15 μL min$^{-1}$ oil sample and 600 μL min$^{-1}$ post-dilution with toluene. If the characteristic absorbance of the filtrate was recorded as 0.300 au (600–800 nm), then the value used in eqn (1) would be 0.337 au based on the 1.122 dilution adjustment to an $R = 40$ equivalent. The dilution normalization is calculated based on the ratio of flow rates for $R = 5$ to $R = 40$; dilution norm. = (75 μL min$^{-1}$ + 15 μL min$^{-1}$ + 600 μL min$^{-1}$)/(15 μL min$^{-1}$ + 600 μL min$^{-1}$) = 1.122. If desired, fractional precipitation values $x(R)$ at each ratio can be converted to weight percentages using the maximum asphaltene absorbance and the correlation in ref. 20. The process of creating a yield curve is graphically summarized in Fig. 2.

## Results and discussion

### Obtaining the yield curve from raw data

The yield curve for an individual crude oil sample is generated by sweeping through a range of heptane–oil ratios and measuring the optical absorbance of the filtrate. Ten to twenty individual experimental runs are performed per yield curve. A subset of the data generated by the microfluidic system for crude oil-A is shown in Fig. 3. The data shows the optical absorbance and pressure profiles plotted *versus* time

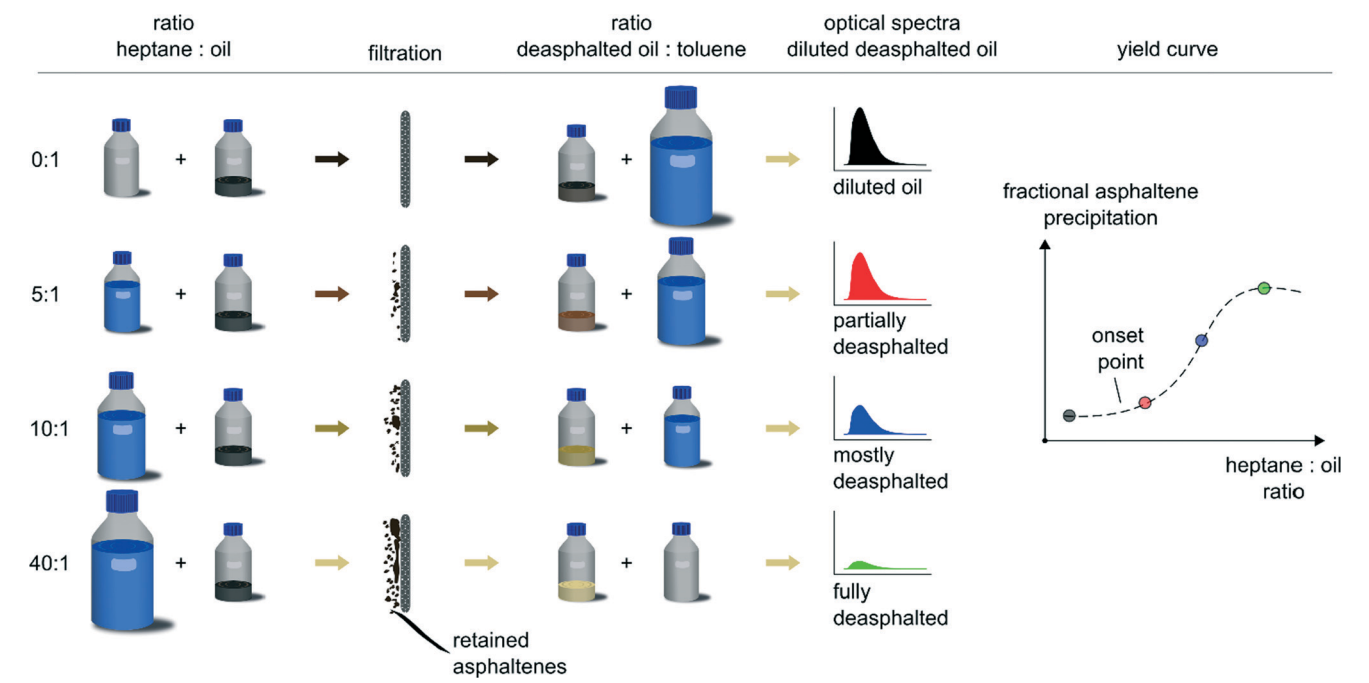


Fig. 2 Schematic of the experimental procedure for acquiring the asphaltene yield curve on the microfluidic device.

for 6 different ratios. At a heptane–oil ratio of 0.25 (labelled "<asphaltenes onset"), the pressure profile shows a gradual increase and decrease as the oil plug passes through the filter membrane. The step drop and rise in pressure that occurs every 550 seconds are the automated syringe refills, also synchronized with the absorbance transients. The absence of stochastic pressure spikes throughout the filtration process indicates that solvent-induced asphaltene aggregation has not yet occurred. The heptane–oil filtrate is then diluted with toluene and an optical absorbance measurement is performed. The average absorbance of the diluted filtrate at the plateau is 0.736 au.

In order to determine if the asphaltenes precipitated at the dilution ratio of 0.25, the absorbance of the toluene-diluted filtrate is compared with the absorbance of the neat oil diluted with toluene ($R$ = 0). The measured absorbance of the toluene-diluted neat oil was 0.800 au. Although the difference in absorbance (0.064 au) indicates that asphaltenes precipitate at the dilution ratio of 0.25, this may be in fact due to the presence of pre-existing asphaltene aggregates in the neat oil. It is worthwhile to note that the absorbance for neat oil is measured by pre-diluting the oil sample with toluene. In the pre-dilution experiment, the oil was mixed with toluene before filtration by injecting toluene instead of heptane at the chip inlet. The addition of toluene before filtration increased the solubility of the mixture and dissolved any suspended asphaltene aggregates. The mixture was then passed through the filter membrane and an absorbance of 0.800 au was measured ($R$ = 0). A post-dilution experiment was conducted as well using the lowest heptane–oil ratio run

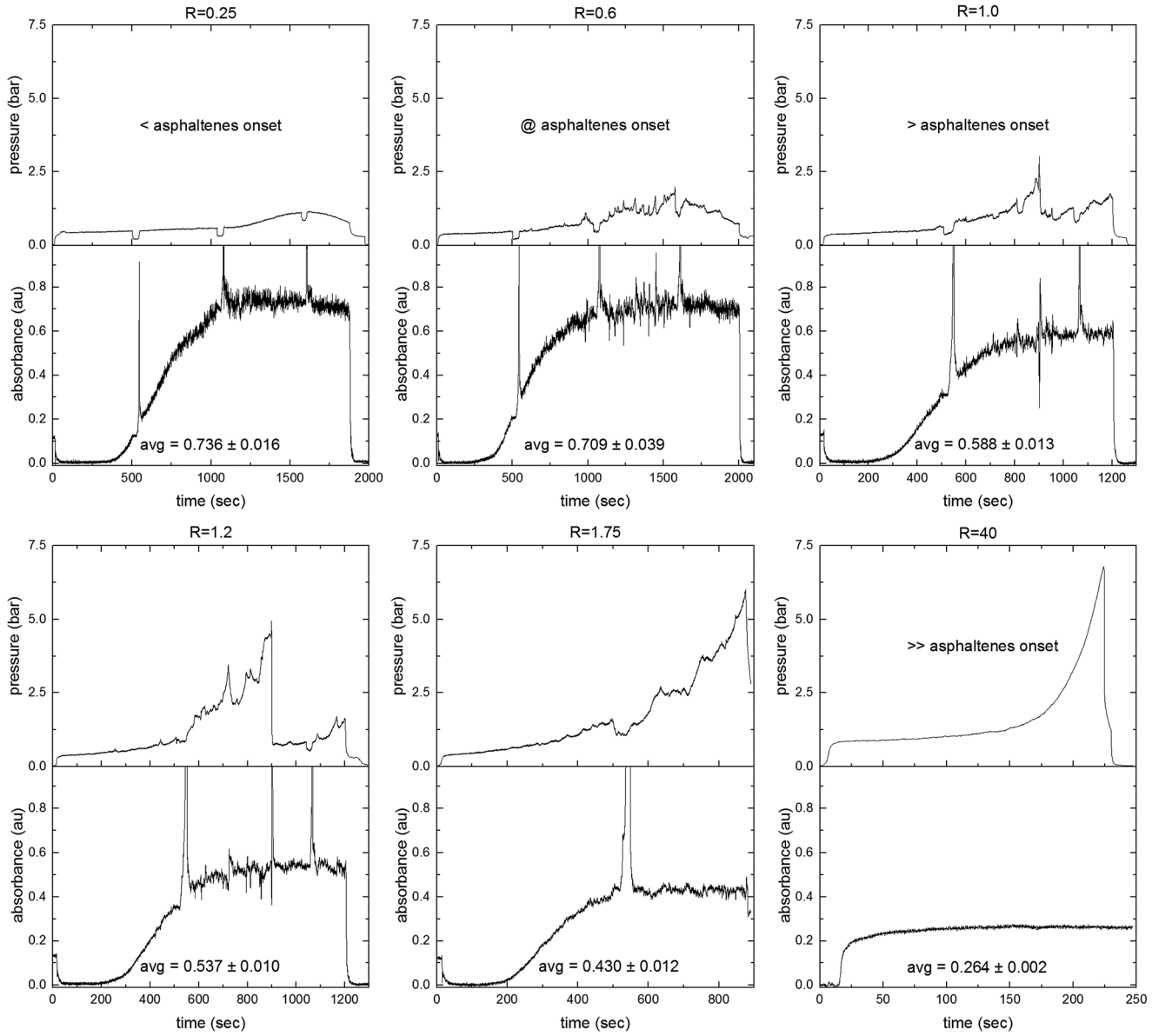


**Fig. 3** Raw data produced by the microfluidic apparatus for crude oil-A. Chip inlet pressure and optical absorbance (600 nm minus 800 nm) *versus* time for various heptane–oil ratios.

 

($R$ = 0.01). In this case, the volumetric flow rates of oil and *n*-heptane were 50 μL min$^{-1}$ and 0.5 μL min$^{-1}$, respectively. The heptane–oil mixture was filtered and then post-diluted with toluene to perform an absorbance measurement. The filtrate had an absorbance of 0.760 au. At a low heptane volume concentration of 1%, the addition of *n*-heptane is unlikely to induce asphaltene precipitation. Post-dilution with toluene was also performed at the heptane–oil ratio of 0.05. A similar absorbance of 0.760 au was observed. Hence, the difference between the pre-dilution and post-dilution absorbance values at low dilution ratios suggest the presence of pre-existing asphaltene aggregates in the neat oil. Crude oil-A was the only sample in this dataset that showed a difference between pre-dilution with toluene ($R$ = 0.0) and post-dilution with toluene ($R < 0.05$). As a result, we modified the microfluidic method to use the pre-diluted run/case as the zero precipitation absorbance value to account for the presence of suspended aggregates.

Fig. 3 shows that solvent-induced asphaltene onset was detected between the heptane–oil ratios of 0.6 and 1.0 for crude oil-A, labelled "@ asphaltenes onset". The aggregation of asphaltenes is first detectable at $R$ = 0.6, noted by the combined effects of a drop in steady-state absorbance and the fluctuating pressure pattern. The absorbance of the filtrate decreased from 0.736 au ($R$ = 0.25) to 0.709 au ($R$ = 0.6). Also, the absorbance standard deviation on the plateau was 0.039 au at $R$ = 0.6, which is the largest of all heptane–oil ratios. Typically, we observe a standard deviation of less than 0.015 au for the plateau measurement. This may indicate that the size of the asphaltene aggregate is slightly below the 0.2 μm filter pore size. A fraction of the particles are small enough to pass through the filter, but large enough to result in light scattering as they pass through the optical flow cell.[6] Additionally, at the onset we often noted a rising pressure profile with momentary spikes in pressure as the heptane–oil filtrate passed through the membrane. The fluctuating pressure patterns arose from asphaltene aggregates clogging the filtration microchannel as the membrane filtered and collected asphaltenes on the topside open face channel. At low ratios, the clogs occurred at the start of the of the filtration channel just after the reactor. Pressure build-ups from the continuously flowing viscous heptane–oil mixture would dislodge and clear these channel blockages, sweeping the aggregates to the end of the filtration channel. The repeating pattern of block-pressurize-dislodge-block produced large pressure transients at low ratios. When the heptane–oil ratio was increased above the asphaltene onset ($R$ = 1.0 to $R$ = 1.75), the pressure rise started earlier, was more systematic and was higher in magnitude. More asphaltenes were precipitated and filtered, leading to a greater degree of membrane fouling and a rise in pressure. The increase in system pressure, which was due to mixer clogging as well as membrane fouling, was tolerated up to 6 bars, beyond which the system was automatically stopped. The precipitated asphaltenes in the microchannels and the membrane were then dissolved using toluene. The removal of asphaltenes from the crude oil also produced a lower filtrate absorbance of 0.588 au, 0.537 au and 0.430 au for the heptane–oil ratios of 1.0, 1.2 and 1.75, respectively.

At higher heptane–oil ratios ($R > 2$), the precipitant driving force is sufficient for rapid aggregation. When heptane was added in excess to the oil, $R$ = 40 (labelled "≫asphaltenes onset") – Fig. 3, an early pressure rise was observed with a low characteristic absorbance of 0.264 au. The smooth and rapid pressure rise was attributed to a systematic dead-end filling of the filtration channel with asphaltenes as the heptane–oil mixture was filtered.

After gathering data for the desired number of heptane–oil ratios, the optical absorbance spectra were processed to produce the fractional yield data as shown in Fig. 4A as per eqn (1). Specifically, the asphaltene absorbance for each heptane–oil ratio was calculated by subtracting the filtrate absorbance at that heptane–oil ratio from the absorbance of the neat oil (pre-diluted with toluene, $R$ = 0). The asphaltene absorbance value for each heptane–oil ratio was then normalized to the asphaltene absorbance at the maximum precipitation to obtain the fractional precipitation yield.

### Comparison of conventional and microfluidic methods

The microfluidic yield data is compared to conventional yield data for oil-A and oil-B, shown in Fig. 4A and B, respectively. Conventionally measured yield data for crude oils A and B were published in ref. 36. Oil-A microfluidic data showed a reasonable agreement with the conventional data, compared in Fig. 4A. The asphaltene onsets were similar, with the microfluidic onset at a heptane–oil ratio of 0.6 and the conventional onset at 0.5. As the heptane percentage was increased in the mixture, both microfluidic and conventional yield data showed similar front-ends: a steep rise, then a levelling-off point at a heptane–oil ratio of 3, followed by a shallow rise to the maximum precipitation. However, for heptane–oil ratios greater than 30, there was a slight deviation; the microfluidic data tended downward while the conventional data showed a plateau. We discuss the microfluidic downward trend under the section of infinite dilution below. The data for crude oil-B in Fig. 4B showed asphaltene onsets that were nearly identical at a ratio between 2.0 to 2.5. In this example, the conventional data had a more gradual rise to the maximum precipitation compared to the microfluidic measurements. A large degree of scatter after a heptane–oil ratio of 20 for the conventional measurements makes it difficult to precisely determine the maximum precipitation yield. For both crude oils A and B, the conventional gravimetric data and the microfluidic optical data are similar in precipitation onset and curve shape.

The slightly higher microfluidic onset compared to the conventional onset for oil-A, 0.6 *versus* 0.5, may result from the microfluidic method over-estimating the solubility of asphaltenes at low ratios ($R < 2$). Maqbool *et al.* demonstrated that near asphaltene precipitation onset ($R \approx 0.5$–2), the aggregation process may take time from minutes to

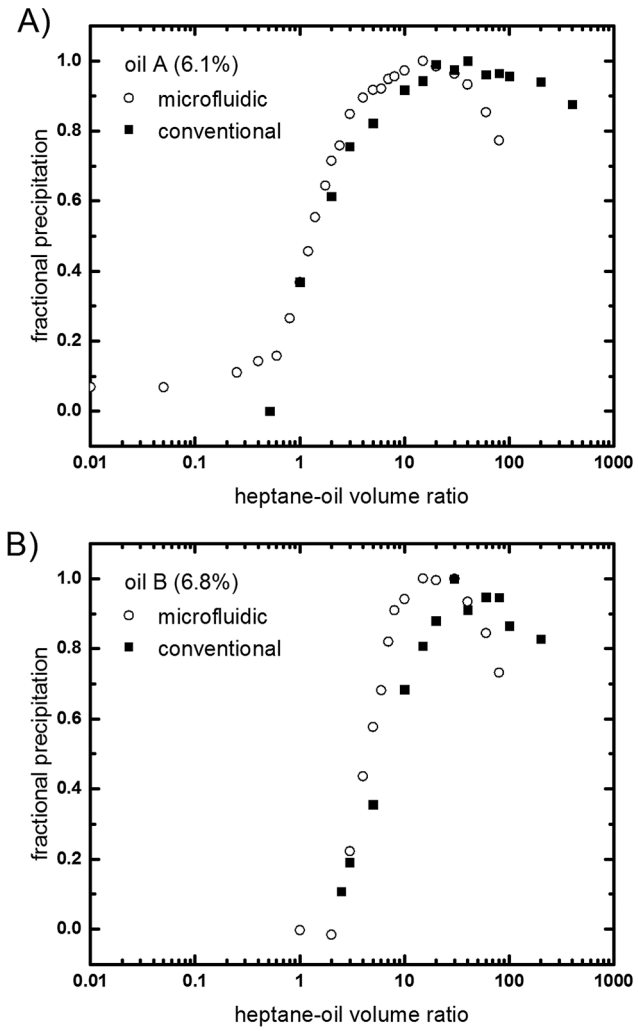


Fig. 4 Comparison of asphaltene yields measured from conventional and microfluidic methods. The traditionally measured maximum asphaltene content of the oil samples (in wt%) is provided in brackets.

thousands of hours, depending on the crude oil.[39] In their work, detection of precipitation onset was based on the observation of particles greater than 0.5 μm using light microscopy. Maqbool *et al.* studied two oils and showed that the precipitation onset was only detectable after 1000–5000 hours for a heptane volume of ~40% ($R$ = 0.67). However, with a slightly higher heptane volume of ~55% ($R$ = 1.22), one of the oils had noticeable precipitation in less than a minute. The other oil required a heptane volume of ~60% ($R$ = 1.50) to induce precipitation within minutes. The study highlights the importance of aggregation kinetics in detecting asphaltene precipitation onset – there is an exponential dependence on particle formation rate and precipitant concentration. In our study, the slower flow rates used at low heptane–oil ratios provide increased residence time in the reactor channel of the chip. The time for asphaltene aggregation on the chip ranges from 30 seconds ($R$ = 0.4) to 0.5 seconds ($R$ = 80). Therefore, the microfluidic method is likely over-estimating the solubility of asphaltenes near onset by not providing enough time for aggregates to grow. Asphaltene precipitation onset may physically occur at slightly lower heptane–oil ratios than our measured onsets. Longer time delays in the reactor channel or smaller filter pore-sizes (~10–50 nm) could be used to improve the detection of precipitation onset. Even when considering the kinetics effects, the 0.1 difference between onsets is within experimental error.

### Sample set yield data

The precipitation yield data for crude oils A, B and C are shown in Fig. 5A. Fractional precipitation is plotted *versus* heptane–oil volume ratio. The samples in Fig. 5A are shown together to highlight that the onset point, general shape and maximum precipitation are easily discernible and different for each oil sample as measured by the microfluidic method. To evaluate the lower and upper operational limits of the microfluidic method, yield data for crude oils D and E are also shown in Fig. 5B and C. For the waxy crude, oil-F, measurements are performed at 65 °C and the yield data is shown in Fig. 5D.

The yield curve in Fig. 5B was acquired from the relatively low asphaltene content oil – crude oil-D with an asphaltene content of 1.1 wt%. A total of 19 microfluidic experiments were conducted at room temperature, 22–24 °C, with varied heptane–oil ratios ranging from 0 to 80. As expected, at low heptane concentration ($R < 0.6$), the fractional precipitation was virtually zero. At a heptane–oil ratio of 0.6, the first portion of asphaltene aggregates form and were separated by the porous membrane; therefore, we consider the heptane–oil ratio of 0.6 as the onset point (similar to the method above). As the percentage of heptane increased after the onset point, so did the amount of precipitated asphaltenes. The asphaltene yield reached a maximum value at a heptane–oil ratio of 40, beyond which the precipitated amount decreased slightly. This decrease can be associated with an increase in solubility of the asphaltenes in heptane at infinite dilutions, where aggregate formation is hindered by relatively large asphaltene intermolecular distances.[4,40] Heptane–oil ratios greater than the maximum were selected to ensure that the maximum precipitation was measured and to investigate the decline after the peak. The optical setup used here was limited to a heptane–oil ratio of approximately 100, where the diluted oil absorbance signal was typically outside the viable measurement range and approached the system's noise limits. Longer optical path lengths may be used to measure the precipitation yield for heptane–oil ratios beyond 100.

Two technical problems were encountered when acquiring the yield curve for crude oil-D. First, when unfiltered oil was analyzed with the microfluidic system, the transmembrane pressure exceeded 6 bar; thereby making steady state optical readings difficult to obtain. This only occurred for very low mixing ratios. However, when the oil sample was pre-filtered with a 0.2 μm PTFE syringe filter, the maximum observed pressure was reduced sufficiently to permit data collection at

 

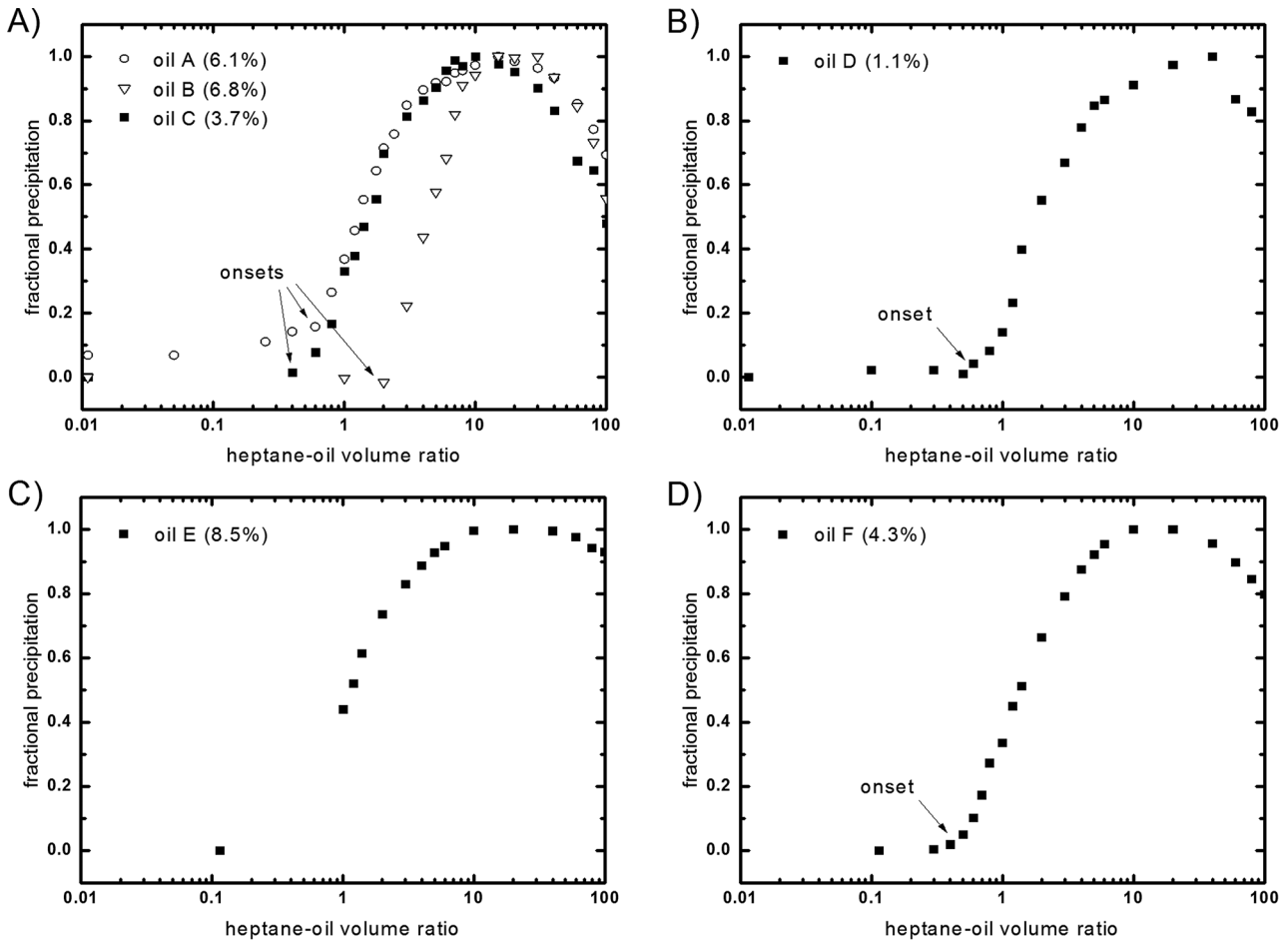


**Fig. 5** Microfluidic system-measured asphaltene yield curves for the six crude oils used in this study. The maximum asphaltene content for each oil is provided in brackets. All data acquired at 22–24 °C and 1 atm, with the exception of crude oil-F performed at 65 °C and 1 atm.

low heptane–oil ratios ($R < 5$). This suggests that the crude oil-D sample had notable fines and/or precipitated wax that led to early membrane clogging. Samples that produce significant transmembrane pressures, greater than 5 to 6 bar, should be pre-filtered to remove the particulate matter. If the pressure build-up resulted from wax, temperatures above the wax appearance temperature can be used for measuring the yield curve. In either case, pre-filtration using the same pore size and removal of particulate matter, such as wax or fines, did not impact the measured optical absorbance. Second, the system dead-volume (152 μL) became appreciable at low mixing ratios. For example, at a heptane–oil ratio of 1, a total volume of 400 μL (200 μL heptane + 200 μL oil) was delivered to the system and Taylor dispersion led to more pronounced sample smearing.[41] This reduced the duration of the optical measurement plateau and in some cases the absorbance signal did not reach steady-state. To achieve a suitable measurement window, it was necessary to increase the injected sample volume from 200 μL to 500 μL. This solution had two detrimental effects: a) it increased the amount of the oil sample and more asphaltenes were deposited on the filter membrane, and b) it made the experimental runs at least 2.5 times longer. At slow flow rates near onset ($R < 2$), this was amplified as it took longer to displace the chip's dead-volume and reach a steady-state; experimental times were approximately 2000 seconds ($R \approx 0$) instead of 200 seconds ($R > 10$). Although this solved the dead-volume problem for crude oils A–D, samples with higher asphaltene content will not benefit from this solution as the filtration channel may completely fill before the system reaches steady-state.

Fig. 5C depicts the yield curve (15 experiments) for the highest asphaltene content sample, crude oil-E, at 8.5 wt%. The maximum precipitation was at a heptane–oil ratio of 20. Crude oil-E showed a more pronounced leveling off unlike crude oils A–D, as the fractional precipitation differed by less than 0.5% at heptane–oil ratios of 10, 20 and 40. The precipitation onset could not be readily measured for this sample because the apparatus over-pressured before reaching a stable measurement plateau. Even with a larger filter pore size of 1.2 μm, rapid clogging occurred for heptane–oil ratios lower than 5 and prevented a steady-state measurement below a heptane–oil ratio of 1. A redesigned chip with a large filtration capacity channel would address this limitation for high asphaltene content crude oils. Fundamentally, we do not anticipate any issues for low or high asphaltene content oils between the microfluidic and conventional approaches.

The final crude oil sample, oil-F with an asphaltene content of 4.3 wt% and an appreciable wax content was analyzed. A wax appearance temperature of 32.2 °C was measured using cross polarization microscopy.[42] Fig. 5D shows the yield curve for this sample measured at 65 °C for heptane–oil ratios ranging from 0 to 100. In the case of crude oil-F, the precipitation temperature was chosen at 65 °C *versus* 22–24 °C to avoid filter membrane fouling due to wax deposition. The test at elevated temperature slightly increased the asphaltene solubility, thereby decreasing the precipitation yield and shifting the yield curve. The ability to run solubility analysis at multiple temperatures, for modelling or to evaluate waxy crudes, demonstrates the flexibility of the microfluidic method. The yield curve for this sample exhibited no asphaltene precipitation at low heptane–oil ratios ($R < 0.3$). The precipitation onset occurred at a heptane–oil ratio of 0.4 and the maximum precipitation was at a heptane–oil ratio of 10.

A total of 21 experiments were performed to acquire the yield curve in Fig. 5D, which required 15 hours of experimental time (10% setup, 90% runtime), 0.435 L of solvent and 9.3 mL or 8.2 g of crude oil sample. The operator was only required for a few hours to setup the device. Using conventional methods, approximately 0.3–0.5 L of solvent and 5 g of crude oil are required for each point on the yield curve. An entire yield curve would consume over 6 L of solvent (a conservative estimate) and more than 100 g of crude oil sample based on 20 points. Further, even if multiple runs/ratios were completed in parallel, it would take a trained operator over 5 working days, including drying, to collect all the data in the yield curve.[35] The microfluidic approach results in over an order of magnitude of improvement in solvent use with no loss in data quality, thereby reducing the environmental footprint of such measurements.

### Infinite dilution effect

Generally, the microfluidic yield curve data showed a consistent downward trend at high heptane–oil ratios, observed in varying degrees for the six oil samples used in this study. Two main factors contribute to the differences in asphaltene yield at high dilution ratios obtained between the conventional and microfluidic methods.

First, both methods suffer from diminished signal-to-noise ratios (SNRs) at high heptane dilutions. For gravimetrically measured yield data, either vast volumes of solvent or small sample masses must be used to achieve such high dilution ratios. Hence, conventional approaches introduce error *via* manual dilution and washing steps or by mass measurement limits. For optically measured yield curves, the high dilution ratios produce a fluid with substantially low absorption of light. The optical path length of a system is usually fixed and designed for a specific dynamic range. The range is constrained by the Beer–Lambert law assumptions and by detector sensitivity; often targeted for measuring an absorption of less than 2 au and above the inherent detection noise.[38] In the described system, the standard deviation on a blank measurement was typically ± 0.005 au and the standard deviation on a sample measurement was often ±0.015 au. The limit-of-detection (LOD) can be defined as 3 times the standard deviation of a blank measurement, which leads to an LOD of ±0.015 au. For crude oil-F (Fig. 5D), a heptane–oil ratio of 60 produced a filtrate absorbance of 0.212 au. Applying the standard deviation of 0.015 au leads to an absorbance range of 0.197–0.227 au. The fractional precipitation at $R$ = 60 was 89.7% (0.212 au) and based on the standard error in absorbance, it ranges from 86.1% (0.227 au – less apparent asphaltene filtration) to 93.4% (0.197 au – more apparent asphaltene filtration), or ±3.7% in the fractional precipitation. At higher dilution ratios ($R > 100$), this error becomes more pronounced as the optical absorbance values approach and become comparable to the LOD.

Second, at high dilution ratios, diffusion limited aggregation (DLA) becomes dominant and the significance of asphaltene aggregation kinetics is reduced, or reaction-limited aggregation (RLA) is less dominant. This is important at high heptane–oil ratios because the residence time for the precipitated asphaltenes in the microfluidic reactor is relatively short. For example, the residence time is about 0.5 seconds for a heptane–oil ratio of 80, while the residence time is about 13 seconds at a heptane–oil ratio of 5. Therefore, the aggregates may not have enough time to grow in size beyond the nominal 200 nm filter pore size. Conversely, conventional yield experiments are left for several hours and can be incubated for days or even months, providing sufficient time for aggregation to take place and form adequately sized aggregates.[36,39,43–45] Although microchannel mixing processes are much more rapid than conventional bulk mixing approaches,[37] DLA may become problematic at exceedingly high dilution ratios. One potential work around would be the implementation of a stop-flow type system with a hold chamber that would allow for user-specified long incubation times.[41]

Although there are differences between conventional and microfluidic yield data at high dilution ratios, a downward trend may be expected where asphaltenes remain largely dissociated due to infinite dilution. A modified regular solution model described in Appendix A and ref. 5, 18 and 46 was used to compare the modelled yield curve against the microfluidic yield data, as shown in Fig. 6. The experimental microfluidic data closely captures the shape of the model yield curve, including the downward trend at high dilution ratios. The model inputs are the normalised mass fractions of the SARA composition fractions in the crude oil and the average molar mass of self-associated asphaltenes. To cover a wider range of asphaltene molar mass distribution, SARA fractions based on *n*-pentane precipitated asphaltenes are used in the model (C5-asphaltenes) and the average molar mass of asphaltenes is adjusted to fit the measured precipitation onset. The *n*-pentane separated asphaltenes were measured on the microfluidic device as having an optical absorbance of 1.12 times the *n*-heptane separated asphaltenes for crude oil-F at a heptane–oil ratio of 40. As the model required the C5-asphaltenes, we applied the C5/C7 microfluidic

 

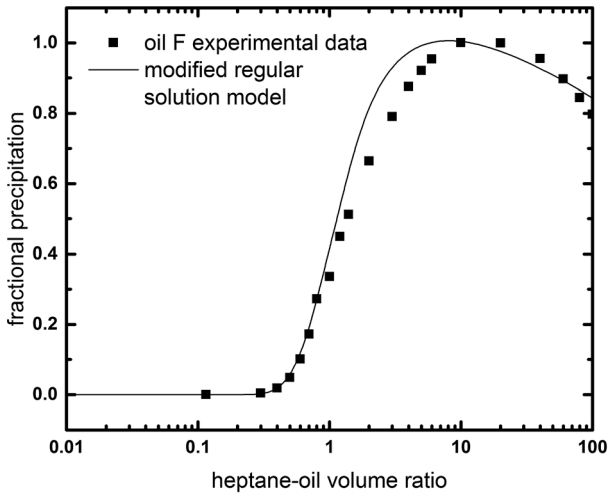


Fig. 6 Asphaltene precipitation yields for crude oil-F at 65 °C and 1 atm, showing the modified regular solution model and microfluidic experimental data.

absorbance ratio to the conventionally measured C7-asphaltenes (4.3 wt%) and removed the differential amount from the resins fraction (0.5 wt%). For crude oil-F, the resulting mass fractions of saturates, aromatics, resins and C5-asphaltenes used in the model are 54.4, 21.9, 18.3 and 4.8 wt%, respectively. The fitted molar mass of asphaltene nanoaggregates in crude oil-F was found to be 3185 g mol$^{-1}$, which compared reasonably well with the average nanoaggregate mass determined for oils from the same geographic location.[19]

We use the term asphaltene nanoaggregates above to describe the self-associated stacks of asphaltene molecules as per the Yen–Mullins model.[47] It must be highlighted that 3185 g mol$^{-1}$ is only a fitting parameter for the modified regular solution model and is best linked to an average nanoaggregate mass and not an average asphaltene molar mass. Wu *et al.* showed asphaltene molecular masses ranging from 580–700 g mol$^{-1}$ and they also determined that petroleum asphaltenes form nanoaggregates that typically contain 6–8 molecules.[47,48] Based on the above model fitting parameter and molar mass range, oil-F could contain approximately 4–5 asphaltenes molecules in a nanoaggregate. Overall, the asphaltene yields obtained from microfluidic system matched the conventionally measured yield data and also follow the model yield trend at high dilutions. We have shown a novel microfluidic approach for determining asphaltene onset point, as well as, fractional precipitation or yield data. The data generated from our device is useful for probing asphaltene solubility in crude oils and for tuning such models, without the long turn-around times of conventional methods.

## Conclusions

In this study, we have introduced a microfluidic apparatus for rapidly obtaining the yield curve for a sample of crude oil. The system is built upon a technique for measuring asphaltenes using optical spectroscopy combined with a microfluidic fluid handling platform. To build each yield curve, tens of asphaltene solubility measurements in heptane are completed in one day instead of the several weeks to months required by conventional approaches. The microfluidic system also produced 10-fold less waste, oil and solvent, making the system portable and more cost-effective for such resource intensive studies. We have shown that the precipitation onset and maximum precipitation can be determined from the data and that regular solution models can be tuned to model the data reasonably well. Generally, such microfluidic systems will enable fast, accurate, repeatable and cost-effective solubility measurements for tuning petroleum processes and models.

## Appendix A. Modified regular solution model

The details of the model have been presented elsewhere.[5,46] Briefly, the modified regular solution model includes a Flory–Huggins entropic contribution from the difference in molecular sizes as well as an enthalpy contribution from regular solution or Scatchard-Hildebrand solubility theory. A liquid–liquid equilibrium is assumed and the equilibrium ratio, $K_i^{\mathrm{hl}}$, for any given component is given by:

$$K_i^{\mathrm{hl}} = \frac{x_i^{\mathrm{h}}}{x_i^{\mathrm{l}}} = \exp\left\{\begin{array}{l} \dfrac{v_i^{\mathrm{h}}}{v_{\mathrm{m}}^{\mathrm{h}}} - \dfrac{v_i^{\mathrm{l}}}{v_{\mathrm{m}}^{\mathrm{l}}} + \ln\left(\dfrac{v_i^{\mathrm{l}}}{v_{\mathrm{m}}^{\mathrm{l}}}\right) - \ln\left(\dfrac{v_i^{\mathrm{h}}}{v_{\mathrm{m}}^{\mathrm{h}}}\right) \\ + \dfrac{v_i^{\mathrm{l}}}{RT}\left(\delta_i^{\mathrm{l}} - \delta_{\mathrm{m}}^{\mathrm{l}}\right)^2 - \dfrac{v_i^{\mathrm{h}}}{RT}\left(\delta_i^{\mathrm{h}} - \delta_{\mathrm{m}}^{\mathrm{h}}\right)^2 \end{array}\right\} \quad \text{(A1)}$$

where $x_i^{\mathrm{h}}$ and $x_i^{\mathrm{l}}$ are the heavy and light liquid phase mole fractions, $R$ is the universal gas constant, $T$ is the absolute temperature, $v_i$ and $\delta_i$ are the molar volume and solubility parameter of component $i$ in either the light liquid phase ($l$) or the heavy liquid phase ($h$), and $v_{\mathrm{m}}$ and $\delta_{\mathrm{m}}$ are the molar volume and solubility parameter of either the light liquid phase or the heavy liquid phase. The terms containing only molar volumes are the entropic contribution and the terms containing solubility parameters are the enthalpic contribution.

Once the equilibrium ratios are known, the phase equilibrium calculations are performed using standard techniques to determine the composition and amounts of heavy and light liquid phases. The amount of heavy liquid phase is considered as the amount of asphaltenes precipitated. To use this model, the mole fraction, molar volume, and solubility parameter of each component in the mixture must be specified. The molar volume is obtained from molar mass and density. In this study, the heptane–oil mixture is characterized into five components: *n*-heptane, saturates, aromatics, resins and asphaltenes. Pure component properties are used for *n*-heptane and average properties are used for SARA fractions. The generalized molar mass and property (density and solubility parameter) correlations for the SARA fractions can be found elsewhere.[19]

The modified model also treats the asphaltenes as macromolecular nanoaggregates of monodispersed monomers.

Hence, the asphaltene pseudo-component is divided into 30 sub-fractions, each representing a different aggregate size and the number of monomers in an aggregate or the aggregation number ($r$) is described by the relation:

$$r = \frac{M}{M_m} \quad \text{(A2)}$$

where $M$ is the molar mass of the particular asphaltene aggregate or the sub-fraction, and $M_m$ is the monomer molar mass of the asphaltenes. The gamma distribution function[49] is then used to describe the molar mass distribution of the aggregates according to the following equation:

$$f(M) = \frac{1}{M_m \Gamma(\beta)} \left[ \frac{\beta}{(\bar{r} - 1)} \right]^{\beta} \times (r-1)^{\beta-1} \exp\left[ \frac{\beta(1-r)}{(\bar{r}-1)} \right] \quad \text{(A3)}$$

where $\bar{r}$ is the average aggregation number of asphaltene fraction defined as the average molar mass of all self-associated asphaltene sub-fractions ($\bar{M}$) divided by the monomer molar mass, that is given by $\frac{\bar{M}}{M_m}$. $\beta$ is a parameter that determines the shape of the distribution. The value of $\beta$ is chosen as 3.5 based on an extensive data set. The molar mass of an asphaltene monomer and the largest asphaltene aggregate are assumed to be 1800 and 30 000 g mol$^{-1}$, respectively. Note that the asphaltene monomer molar mass of 1800 g mol$^{-1}$ may represent an already aggregated component. Therefore, the only other input to the model is the average molar mass of all self-associated asphaltene sub-fractions ($\bar{M}$).

## Acknowledgements

We would like to acknowledge Professor Harvey Yarranton, Dr. Kamran Akbarzadeh, Dr. Simon Andersen and Dr. Shawn Taylor for providing guidance and assistance with asphaltene solubility. In addition, we note our many insightful remarks and discussions on asphaltenes with Laura Magro, Dr. Marc Schneider and Dr. Oliver Mullins. Also, we acknowledge Dr. Jeff Creek and Dr. Jianxin Wang from Chevron for providing crude samples.

## References

1 O. C. Mullins, *et al.*, *Asphaltenes, Heavy Oils, and Petroleomics*, Springer, 2007.
2 J. G. Speight, *The Chemistry and Technology of Petroleum*, Taylor & Francis, 1999.
3 D. Eskin, *et al.*, Modeling of asphaltene deposition in a production tubing, *AIChE J.*, 2012, **58**(9), 2936–2948.
4 K. Akbarzadeh, *et al.*, Methodology for the characterization and modeling of asphaltene precipitation from heavy oils diluted with n-alkanes, *Energy Fuels*, 2004, **18**(5), 1434–1441.
5 H. Alboudwarej, *et al.*, Regular Solution Model for Asphaltene Precipitation from Bitumens and Solvents, *AIChE J.*, 2003, **49**(11), 2948–2956.
6 A. Hammami, *et al.*, Asphaltene precipitation from live oils: An experimental investigation of onset conditions and reversibility, *Energy Fuels*, 2000, **14**(1), 14–18.
7 J. X. Wang, *et al.*, A practical method for anticipating asphaltene problems, *SPE Prod. Facil.*, 2004, **19**(3), 152–160.
8 E. Rogel, C. Ovalles and M. Moir, Asphaltene stability in crude oils and petroleum materials by solubility profile analysis, *Energy Fuels*, 2010, **24**(8), 4369–4374.
9 I. A. Wiehe, Asphaltene solubility and fluid compatibility, *Energy Fuels*, 2012, **26**(7), 4004–4016.
10 I. A. Wiehe and R. J. Kennedy, Oil compatibility model and crude oil incompatibility, *Energy Fuels*, 2000, **14**(1), 56–59.
11 G. L. Oliensis, A qualitative test for determining the degree of heterogeneity of asphalts, *Am. Soc. Testing and Materials Proc.*, 1933, vol. 33(2), pp. 715–728.
12 M. H. Schneider, *et al.*, Asphaltene molecular size by fluorescence correlation spectroscopy, *Energy Fuels*, 2007, **21**(5), 2875–2882.
13 P. Fotland, H. Anfindsen and F. H. Fadnes, Detection of asphaltene precipitation and amounts precipitated by measurement of electrical conductivity, *Proceedings of the 6th International Conference on Fluid Properties and Phase Equilibria for Chemical Process Design 1992*, 1993, vol. 82(pt 1), pp. 157–164.
14 A. K. M. Jamaluddin, *et al.*, Laboratory techniques to measure thermodynamic asphaltene instability, *J. Can. Pet. Technol.*, 2002, **41**(7), 44–52.
15 J. Escobedo and G. A. Mansoori, Viscometric determination of the onset of asphaltene flocculation: A novel method, *SPE Prod. Facil.*, 1995, **10**(2), 115–118.
16 A. M. Kharrat, *et al.*, Issues with comparing SARA methodologies, *Energy Fuels*, 2007, **21**(6), 3618–3621.
17 O. Sabbagh, *et al.*, Applying the PR-EoS to asphaltene precipitation from n-alkane diluted heavy oils and bitumens, *Energy Fuels*, 2006, **20**(2), 625–634.
18 A. K. Tharanivasan, *et al.*, Measurement and modeling of asphaltene precipitation from crude oil blends, *Energy Fuels*, 2009, **23**(8), 3971–3980.
19 A. K. Tharanivasan, H. W. Yarranton and S. D. Taylor, Application of a regular solution-based model to asphaltene precipitation from live oils, *Energy Fuels*, 2011, **25**(2), 528–538.
20 M. H. Schneider, *et al.*, Measurement of Asphaltenes Using Optical Spectroscopy on a Microfluidic Platform, *Anal. Chem.*, 2013, **85**(10), 5153–5160.
21 C. Hu, J. E. Morris and R. L. Hartman, Microfluidic investigation of the deposition of asphaltenes in porous media, *Lab Chip*, 2014, **14**(12), 2014–2022.
22 S. A. Bowden, *et al.*, The liquid-liquid diffusive extraction of hydrocarbons from a North Sea oil using a microfluidic format, *Lab Chip*, 2006, **6**(6), 740–743.
23 S. A. Bowden, *et al.*, Determination of the asphaltene and carboxylic acid content of a heavy oil using a microfluidic device, *Lab Chip*, 2009, **9**(6), 828–832.
24 V. Sieben, A. Kharrat and F. Mostowfi, Novel measurement of asphaltene content in oil using microfluidic technology,

 

in *SPE Annual Technical Conference and Exhibition*, ATCE 2013, 2013, New Orleans, LA.
25 C. Hu and R. L. Hartman, High-throughput packed-bed microreactors with in-line analytics for the discovery of asphaltene deposition mechanisms, *AIChE J.*, 2014, **60**(10), 3534–3546.
26 S. Molla, D. Eskin and F. Mostowfi, Two-phase flow of gas-liquid binary mixtures through a rectangular microchannel, in *2011 AIChE Annual Meeting*, 11AIChE, 2011, Minneapolis, MN.
27 S. Molla, D. Eskin and F. Mostowfi, Two-phase flow in microchannels: The case of binary mixtures, *Ind. Eng. Chem. Res.*, 2013, **52**(2), 941–953.
28 F. Mostowfi, S. Molla and P. Tabeling, Determining phase diagrams of gas–liquid systems using a microfluidic PVT, *Lab Chip*, 2012, **12**(21), 4381–4387.
29 R. Fisher, *et al.*, Equilibrium gas-oil ratio measurements using a microfluidic technique, *Lab Chip*, 2013, **13**(13), 2623–2633.
30 M. Abolhasani, *et al.*, Automated microfluidic platform for studies of carbon dioxide dissolution and solubility in physical solvents, *Lab Chip*, 2012, **12**(9), 1611–1618.
31 H. Fadaei, B. Scarff and D. Sinton, Rapid microfluidics-based measurement of CO 2 diffusivity in bitumen, *Energy Fuels*, 2011, **25**(10), 4829–4835.
32 N. S. Kumar Gunda, *et al.*, Reservoir-on-a-Chip (ROC): A new paradigm in reservoir engineering, *Lab Chip*, 2011, **11**(22), 3785–3792.
33 T. W. De Haas, *et al.*, Steam-on-a-chip for oil recovery: The role of alkaline additives in steam assisted gravity drainage, *Lab Chip*, 2013, **13**(19), 3832–3839.
34 A. M. Kharrat, K. Indo and F. Mostowfi, Asphaltene content measurement using an optical spectroscopy technique, *Energy Fuels*, 2013, **27**(5), 2452–2457.
35 ASTM D6560-12, Standard Test Method for Determination of Asphaltenes (Heptane Insolubles) in *Crude Petroleum and Petroleum Products*, ASTM International, West Conshohocken, PA, 2012, www.astm.org, DOI: 10.1520/D6560-12.
36 J. Wang and J. Buckley, Effect of dilution ratio on amount of asphaltenes separated from stock tank oil, *J. Dispersion Sci. Technol.*, 2007, **28**(3), 425–430.
37 N. T. Nguyen and Z. Wu, Micromixers - A review, *J. Micromech. Microeng.*, 2005, **15**(2), R1–R16.
38 V. J. Sieben, *et al.*, Microfluidic colourimetric chemical analysis system: Application to nitrite detection, *Anal. Methods*, 2010, **2**(5), 484–491.
39 T. Maqbool, A. T. Balgoa and H. S. Fogler, Revisiting asphaltene precipitation from crude oils: A case of neglected kinetic effects, *Energy Fuels*, 2009, **23**(7), 3681–3686.
40 J. Morgado, *et al.*, Thermodynamics of interactions at infinite dilution between asphaltenes and a surfactant or crude oil resins, *Energy Fuels*, 2009, **23**(5), 2581–2591.
41 I. R. G. Ogilvie, *et al.*, Temporal optimization of microfluidic colorimetric sensors by use of multiplexed stop-flow architecture, *Anal. Chem.*, 2011, **83**(12), 4814–4821.
42 K. Karan, J. Ratulowski and P. German, Measurement of Waxy Crude Properties Using Novel Laboratory Techniques (SPE 62945), in *2000 SPE Annual Technical Conference and Exhibition*, 2000, Society of Petroleum Engineers, Dallas, Texas.
43 S. Ashoori, *et al.*, Mechanisms of asphaltene aggregation in toluene and heptane mixtures, *J. Jpn. Pet. Inst.*, 2009, **52**(5), 283–287.
44 J. Hung, J. Castillo and A. Reyes, Kinetics of asphaltene aggregation in toluene-heptane mixtures studied by confocal microscopy, *Energy Fuels*, 2005, **19**(3), 898–904.
45 K. Rajagopal and S. M. C. Silva, An experimental study of asphaltene particle sizes in n-heptane-toluene mixtures by light scattering, *Braz. J. Chem. Eng.*, 2004, **21**(4), 601–609.
46 K. Akbarzadeh, *et al.*, A generalized regular solution model for asphaltene precipitation from n-alkane diluted heavy oils and bitumens, *Fluid Phase Equilib.*, 2005, **232**(1–2), 159–170.
47 O. C. Mullins, *et al.*, Advances in asphaltene science and the Yen-Mullins model, *Energy Fuels*, 2012, **26**(7), 3986–4003.
48 Q. Wu, *et al.*, Laser-based mass spectrometric determination of aggregation numbers for petroleum- and coal-derived asphaltenes, *Energy Fuels*, 2014, **28**(1), 475–482.
49 C. H. Whitson, Characterizing hydrocarbon plus fractions, *Soc. Pet. Eng. J.*, 1983, **23**(4), 683–694.